STUDY OF BEAM-SCATTERING EFFECTS FOR A PROPOSED APS ERL UPGRADE *

A. Xiao [†], M. Borland, X. Dong, ANL, Argonne, IL 60439, USA

Abstract

Beam-scattering effects, including intra-beam scattering (IBS) and Touschek scattering, may become an issue for linac-based 4th-generation light sources, such as X-ray free-electron lasers (FELs) and energy recovery linacs (ERLs), as the electron density inside the bunch is very high. In this paper, we describe simulation tools for modeling beam-scattering effects that were recently developed at the Advanced Photon Source (APS). We also demonstrate their application to a possible ERL-based APS upgrade. The beam loss issue due to the Touschek scattering effect is addressed through momentum aperture optimization. The consequences of IBS for brightness, FEL gain, and other figures of merit are also discussed. Calculations are performed using a particle distribution generated by an optimized high-brightness injector simulation.

INTRODUCTION

The Coulomb scattering between particles inside a beam has been widely studied for circular accelerators. They were largely ignored for linacs in the past, since significant effects are not expected for one-pass, low-repetition-rate systems with relatively large beam size. The scattering rate is quite low, and there is not enough time for the beam to develop any noticeable diffusion. The situation has dramatically changed since linac-based 4th-generation light sources are on the horizon. To provide users with synchrotron radiation with unprecedented high brightness, the required linac beam must have extremely low emittance with significant charge and a high repetition rate. To ensure that the machine can be run safely with acceptable beam losses and that the beam quality will be not harmed by IBS, we developed a series of simulation capabilities in `elegant` [1]. They provide the ability to simulate beam-scattering effects for an arbitrarily distributed linac beam with energy variation.

Beam-scattering effects are traditionally separated into two categories, Touschek effect and IBS, based on whether the scattered particles are lost immediately after the scattering event or not, respectively. In the case of IBS, we only see diffusion that leads to increased emittance in 6-D phase space; whereas in Touschek, a single scattering event may result in loss of the scattered particles. Different theoret-

ical approaches are used to calculate the beam size diffusion rate and beam loss rate. In developing our simulation tools, we followed the same path: the widely used Bjorken-Mtingwa's [2] formula is chosen for calculating the emittance growth rate due to the IBS effect, while a combination of Piwinski's formula and Monte Carlo simulation is used for determination beam loss rates and positions.

Both the Bjorken-Mtingwa formula and Piwinski's formula were developed for stored beam, which has constant energy, and both assume a Gaussian bunch. These assumptions are generally invalid for a linac beam. In previous papers [3, 4, 5, 6], we discussed the beam loss issue for a one-pass transport system (Gaussian beam, constant beam energy), and the IBS for a arbitrarily distributed accelerating beam. In this paper, we describe newly developed methods that give us the ability to simulate the beam loss for an arbitrarily distributed linac beam, and summarize the already existing IBS tools. We also give an example application to a possible ERL-based APS upgrade design [7] using a particle distribution generated by an optimized high-brightness injector simulation [8].

A PROPOSED APS ERL UPGRADE

The APS has an eye on building an ERL for a future upgrade. Figure 1 shows the layout of one proposed design. The existing APS ring is used as part of the new machine. Since the radiation shielding of the APS already exists, there is concern about beam loss rate from the high-average-current ERL beam. Also, because of energy recovery, we will find that a small energy deviation generated at high energy may exceed the energy aperture at the end of deceleration, resulting in beam loss. Therefore, a detailed simulation tool that can determine the beam loss rate and the beam loss position precisely is needed.
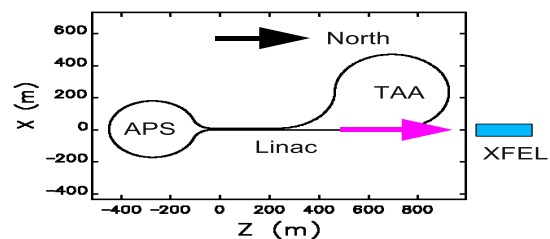

Figure 1: Layout of a proposed APS ERL upgrade.

In general, a linac beam departs from the normally assumed Gaussian distribution that holds for a stored beam,

Multi-Particle Beam Dynamics

especially in the longitudinal dimension. Figure 2 shows the particle distribution from our optimized high-brightness injector simulation. This distribution is used in the later examples of our simulation tools. The major beam parameters of the simulated bunch are: $\varepsilon_{x,n} = \varepsilon_{y,n} = 0.35 \mu m$, $\sigma_p = 2.63 \cdot 10^{-3}$, $\sigma_l = 0.6mm$, bunch charge$= 77pC$, and repetition frequency$= 1.3GHz$.
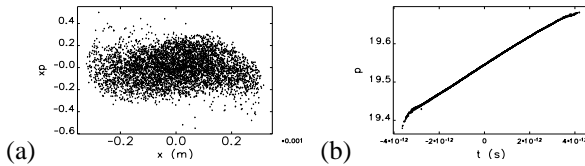

(a)   (b)

Figure 2: Particle distribution from optimized high-brightness injector simulation: (a) horizontal, (b) longitudinal (p=$\beta\gamma$).

TOUSCHEK EFFECT

Simulation of beam loss due to Touschek effect is performed in several steps. The procedure is illustrated in Figure 3. To start the simulation, the beamline under study is first divided into many small sections by inserting a special element `TSCATTER` into it. (This is easily done using the `elegant` command `insert_elements`.) The total number and locations where one should insert `TSCATTER` elements depends on the rapidity with which the energy and optical functions vary. To ensure reliable results, these variations should be small between successive scattering elements.
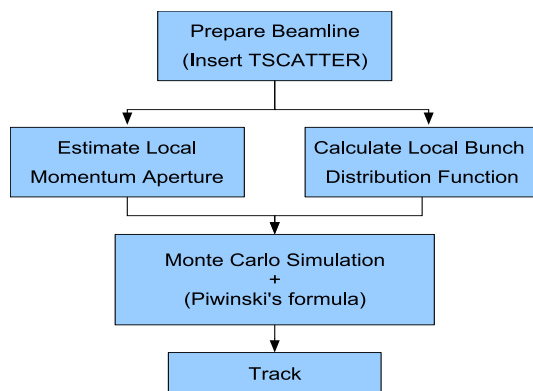

Figure 3: Procedure of the Touschek-caused beam loss simulation.

Estimate local momentum aperture

Unlike in storage rings, the fractional momentum aperture varies over a large range in linacs, as illustrated in Figure 4. In order to efficiently study beam loss from Touschek scattering, we need to know the approximate local momentum aperture and use these results for later simulation [9].

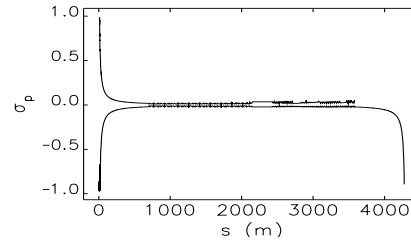`elegant` provides the `momentum_aperture` command to determine local momentum aperture. We also added a

Figure 4: Local momentum aperture for example APS ERL lattice (tracking stopped before last rf module (E=189 MV).

switch in the Touschek simulation module that can generate a momentum aperture bunch at each `TSCATTER` position and then track the bunch to the end of the beamline. The lost particles are collected and an approximate local momentum aperture is obtained. Figure 5 shows an example of the aperture bunch and lost particles.
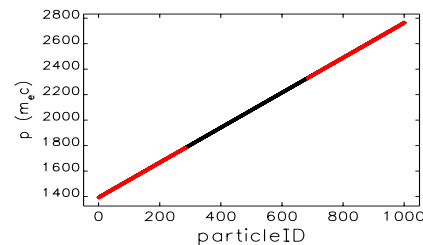

Figure 5: A momentum aperture bunch and lost particles. All particles have $x(x', y, y', t) = 0$.

The results obtained from this step are very important for performing an economical yet detailed Monte Carlo simulation in subsequent steps.

Calculate local bunch distribution function

The electron bunch from a high-brightness injector is typically not Gaussian distributed, especially in the longitudinal direction. As shown in Figure 2, the energy spread of the entire bunch is more than two orders of magnitude larger than the "intrinsic" energy spread. The traditional formulae, which calculate the beam-scattering effect based on the assumption of a Gaussian beam, are therefore invalid. To match our simulation result more closely to the real machine, we track the simulated electron bunch from the gun through the beamline with inserted `TSCATTER` elements. At each `TSCATTER` position, the tracked particles' coordinates are saved so that a corresponding distribution histogram can be made. This distribution histogram (table) is read back later by the Monte Carlo simulation module in order to obtain the particle density by interpolation of the table.

To accomplish this task, we wrote a general tool to generate an n-dimension histogram for a collection of n-tuples, where n can be any integer. Of course, it's natural to build a 6D histogram from a particle distribution. One concern is that, in order to have a meaningful 6D histogram, we need a

huge number of particles from the injector simulation. For example, to have 11 bins in each dimension, the total number of bins is about $11^6 \approx 2 \cdot 10^6$, and the total number of particles need to be larger than this value. Another concern is to interpolate in 6D, any point's value is determined by the nearby $2^6 = 64$ grid point values. This calculation is in principle possible using our software. However, to demonstrate our method in this paper, we separated the beam distribution into two parts: transverse (4D) and longitudinal (2D), see Figure 6. The simulated gun bunch has 500,000 particles.
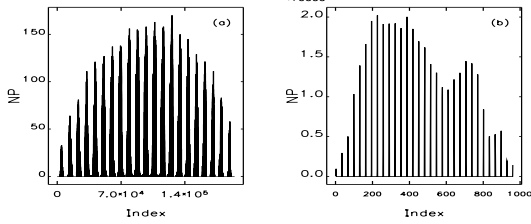

Figure 6: Histogram of the simulated bunch at the beginning of the APS ELR beamline: (a) transverse (4D), (b) longitudinal (2D). (The index is an n-bit counter where each bit has the size of the number of bins of the corresponding dimension.)

Monte Carlo simulation

In the center-of-mass (CM) system [1], the probability of one of the two interacting particles being scattered into a solid angle $d\Omega^*$ is given by the differential Møller cross section [10]

$$\frac{d\sigma^*}{d\Omega^*} = \frac{r_e^2}{4\gamma^{*2}} \left[\left(1 + \frac{1}{\beta^{*2}}\right)^2 \frac{4 - 3\sin^2\Theta^*}{\sin^4\Theta^*} + \frac{4}{\sin^2\Theta^*} + 1 \right],$$
(1)

where r_e is the classical electron radius; γ^* and β^* are the relative energy and velocity of scattered electrons in the CM system, respectively; Θ^* is the angle between the momenta before and after scattering; and $d\Omega^* = \sin\Theta^* d\Theta^* d\Psi^*$.

The Touschek scattered particles' distribution is modeled by Monte Carlo simulation. To use Equation (1), a pair of particles with same position (x, y, t) are generated randomly. Their momenta are transformed into the CM system using the Lorentz transformation. In the CM system, the scattering angles (Θ^*, Ψ^*) are selected randomly. The scattered particles' momenta, together with the associated Møller cross section, are then transformed back to the laboratory coordinate system. Therefore, a single random scattering event includes 11 random numbers (3 positions, 6 momenta, and 2 scattering angles).

The total scattering rate R is given by integral over all possible scattering angles and over all electrons in the

bunch. In the CM system,

$$R^* = 2 \int |v^*| \sigma^* \rho(\vec{x}_1^*)^* \rho(\vec{x}_2^*)^* dV^*,$$
(2)

where v^* is the scattered electrons' velocity, σ^* is the total Møller cross section, $\vec{x}^* = (x^*, y^*, z^*, p_x^*, p_y^*, p_z^*)$, $\rho(x_i^*)^*$ is the electron phase-space density, and $dV = dx^* dy^* dz^* dp_{x1}^* dp_{y1}^* dp_{z1}^* dp_{x2}^* dp_{y2}^* dp_{z2}^*$. σ^* is integrated over the solid angle $d\Omega^*$ with $\Theta^* \in (0, \frac{\pi}{2}]$, $\Psi^* \in [0, 2\pi]$:

$$\sigma^* = \int_0^{2\pi} \int_0^{\pi/2} \frac{d\sigma^*}{d\Omega^*} \sin\Theta^* d\Theta^* d\Psi^*.$$
(3)

The reason for $\Theta^* \in (0, \frac{\pi}{2}]$ is that, if one electron is scattered into the region $0 < \Theta^* \leq \frac{\pi}{2}$, then the other is scattered into the region $\frac{\pi}{2} \leq \Theta^* < \pi$. The factor "2" in Equation (2) includes both regions.

For the problem we are interested in, we assume that $p_x \ll p_z$ and $p_y \ll p_z$, which means that the Lorentz transformation is mainly taking place along the z direction, and σ^* is parallel to the z^*-axis. Transforming to the laboratory coordinate system gives

$$|v|\sigma = \frac{|v^*|}{\gamma} \frac{\sigma^*}{\gamma}$$
(4)

and

$$R = 2 \int |v|\sigma\rho(\vec{x_1})\rho(\vec{x_2})dV,$$
(5)

with

$$dV = dx_\beta dy_\beta d\Delta z dx'_{\beta1} dx'_{\beta2} dy'_{\beta1} dy'_{\beta2} d\Delta p_1 d\Delta p_2.$$
(6)

Equation (5) can be computed using the Monte Carlo integration with N uniform distributed samples in the n-dimensional volume V, e.g.,

$$\int_V f(\vec{x})d\vec{x} \approx \frac{V}{2N} \sum_{i=1}^{M} f(\vec{x_i}),$$
(7)

where "2" represents two particles involved in a sampled scattering event, and the integration is calculated for each scattered particle respectively. For the problem of interest (beam loss calculation), M ($M < 2N$) is the total number of particles with $\delta > \delta_m$, where δ_m is an input value and should be chosen slightly smaller than the local momentum aperture for an economical simulation.

Figure 7 shows the Monte Carlo integration convergence vs. the total number of valid simulated scattered particles M. Based on this, we use $5 \cdot 10^6$ as the default value of M in `elegant`. Figure 8 shows the comparision of the local scattering rates calculated from Piwinski's formula [11] and our Monte Carlo simulation for a Gaussian-distributed beam. We can see that the agreement is excellent.

For a non-Gaussian-distributed beam, `elegant` has the ability to read the real beam distribution function from a
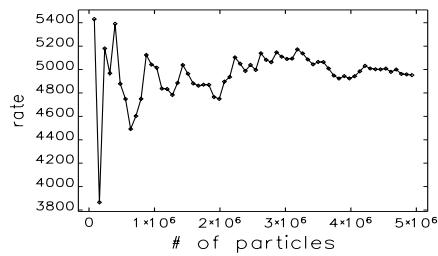
Figure 7: Scattering rate (in an arbitrary scale) vs. number of valid simulated scattered particles.
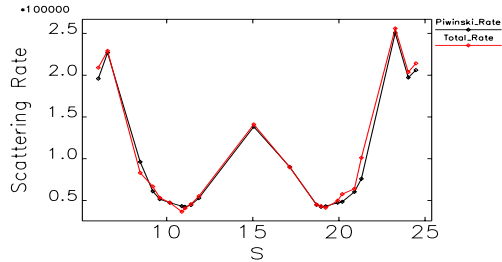

Figure 8: Local Touschek scattering rate (1/s): Piwinski formula (black) and Monte Carlo simulation (red).

histogram table. The table is interpolated to get the values of $\rho(\vec{x_1})$ and $\rho(\vec{x_2})$ in Equation (5). Figure 9 shows the comparison of simulated scattering rate for the assumed Gaussian-distributed beam and the realistic beam distribution. In the dispersion-free regions ($\eta = 0$), we obtained similar results for both cases, which is expected since the transverse beam distribution is very close to the Gaussian distribution. At a location with $\eta \neq 0$, the simulated rate depends on energy spread and the local value of the dispersion. Since the energy distribution is not Gaussian, the results from the Gaussian bunch are unreliable.
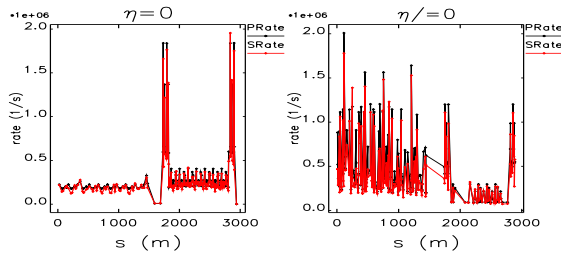

Figure 9: Simulated local Touschek scattering rate (1/s) for Gaussian beam (PRate) and realistic beam distribution (SRate).

Simulation of loss rate and position

Beam-scattering is a random process and can happen at any place along the beamline. The Monte Carlo simulation at one location is already very time consuming. To simulate the Touschek effect at every location of the beamline and obtain a stable statistical result is almost a non-realistic task. From Figure 8, we see clearly that the Monte

Carlo simulation results are very close to Piwinski's formula for a Gaussian-distributed bunch. This fact inspired us to consider using Piwinski's formula to calculate the integrated scattering rate over a section of beamline and using the Monte Carlo simulation to generate random scattered particles. This allows obtaining accurate results with far few particles. Each scattered particle represents a scattering rate of

$$R_i = \frac{r_i}{\sum r_i} \int R_{Piwinski}, \qquad (8)$$

where r_i is the associated local scattering rate $\frac{V}{2N} f(\vec{x_i})$ in Equation (7), $\sum r_i$ is the value of Equation (7), and $\int R_{Piwinski}$ is the integrated Piwinski rate over the section of beamline. For a non-Gaussian-distributed bunch the local scattering rate can not be given by Piwinski's formula. In this case, Equation (8) is modified by multiplying by a factor $\frac{R_{MonteCarlo}}{R_{Piwinski}}$, where $R_{MonteCarlo}$ and $R_{Piwinski}$ are both local rates calculated at the same place.

The scattered particles are then tracked from the scattering location to the end of the beamline. The lost particles R_i and locations are collected, and the total beam loss rate and loss position are given by adding results from all the small beamline sections together.

As shown in Figure 7, to obtain a stable statistical result, the total number of valid events M (*not the total number of samples* $2N$) needs to be large enough. (Recall that M is the number of particles for which $\delta > \delta_m$.) In the case of calculating beam loss rate, it implies that the input value of δ_m should be close to the real momentum aperture for an economical calculation. A value of $0.8\delta_0$, where δ_0 is the estimated momentum aperture, is used in our example simulation.

We examined the scattering rate that each simulated particle represents and, not surprisingly, found a large variation. Some simulated particles represent very likely scattering events, while some represent very low probability events. We sorted all simulated particles by the associated scattering rate. Figure 10 illustrates the sum of the scattering rate ($\sum r_i$) vs. the number of simulated particles ($\sum_i$).
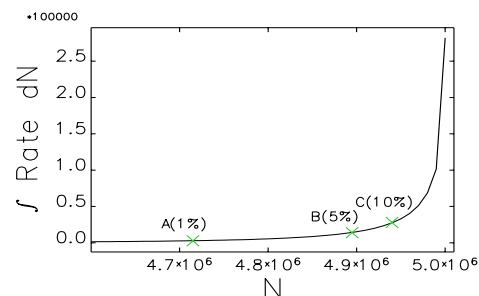

Figure 10: Integrated scattering rate vs. number of simulated particles. Particles are sorted with increasing associated scattering rate.

From this plot we can see that about 5% of simulated particles represent about 99% of the scattering rate. If we
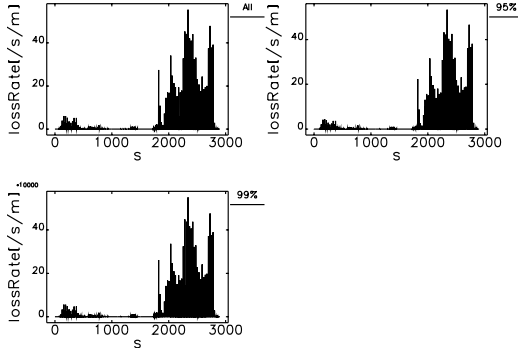
Figure 11: Simulated loss rate vs. position for various values of the scattering rate cut-off.

make use of an estimate of the local momentum aperture, which we do, then a large portion of the simulated particles will be lost somewhere along the beamline. Of those, we need only track that 5% of the particles, which represents 99% of the scattering events. The resulting error will be negligible. Figure 11 compares the computed loss rate for tracking scattered particles with 95%, 99%, and 100% of the total scattering rate, respectively. It's clear that the differences are small. In practice, the user can determine what percentage of scattering they would like to simulate, and elegant will choose the corresponding high-probability scattering events automatically for beam loss study. This strategy makes the calculation even more economical.

An application to the APS ERL upgrade is shown in Figure 12. Without optimized sextupoles installed in the turn-around-arc (TAA) section, the beam loss rate is too high. After optimization of the sextupoles configuration, the beam loss rate in the APS ring portion (from about 2600m to 3600m) is reduced significantly, to a level that is safe for operation.
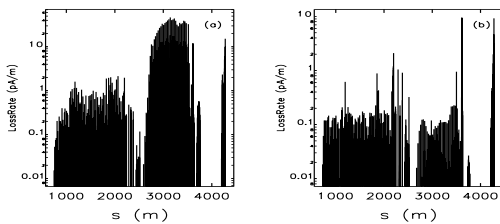

Figure 12: Simulated loss rate vs. position for APS ERL: (a) without sextupole optimization; (b) with optimized sextupoles

IBS EFFECT

The IBS effect is another widely studied beam-scattering effect in storage rings. The emittance growth rate τ_d in the direction d (x, y, or z) is given by the Bjorken-Mtingwa [2] formula for a Gaussian-distributed beam:

$$\frac{1}{\tau_d} = \frac{\pi^2 c r_0^2 m^3 N ln\Lambda}{\gamma \Gamma} f, \tag{9}$$

where c is the speed of light, r_0 is the classical particle radius, m is the particle mass, N is the number of particles per bunch (or in the beam for the unbunched case), $ln\Lambda$ is a Coulomb logarithm, γ is the Lorentz factor, Γ is the 6-dimensional invariant phase-space volume of the beam

$$\Gamma = (2\pi)^3 (\beta\gamma)^3 m^3 \varepsilon_x \varepsilon_y \sigma_p \sigma_z, \tag{10}$$

and f is a complicated function of beam size.

As for the Touschek effect, for a non-Gaussian beam Equation (9) is no longer valid, and we have to search for a new method. Due to the different natures of IBS and Touschek scattering, we care more about beam size evaluation than the real particle distribution, so we choose to continue to use the Bjorken-Mtingwa formula with some modifications. Figure 2 shows that the major difference between a linac beam and a Gaussian beam is in the longitudinal direction. The "intrinsic" energy spread σ_p is much smaller than the bunch's energy spread, and

$$\frac{1}{\tau_d} \propto \frac{1}{\gamma \varepsilon_{xN} \varepsilon_{yN} \sigma_p \sigma_z} f. \tag{11}$$

This difference could result in many orders of magnitude error in the computation of τ_d and must be taken into account. In elegant we provide a slice method to overcome the problem.

First, the beamline is divided into several sections by inserting a special element ISCATTER in the beamline, similar to what we did in the Touschek simulation. Unlike the Touschek simulation, it is not necessary to put as many ISCATTER elements as TSCATTER elements along the beamline, due to the fact that IBS effects need time to develop. An IBSCATTER element is only needed when beam size has a noticeable change due to the IBS effect.

For each section of beamline, the bunch is sliced longitudinally at the beginning of the section. The beam parameters and optical functions are calculated for each slice and propagated to the end of the section. To deal with a bunch traveling through a linac with energy variation, normalized beam parameters are used and are assumed to be unchanged for each section. Because there are no synchrotron oscillations for a linac bunch, the longitudinal growth rate is increased by a factor of 2 based on Piwinski's [12] formula

$$\frac{1}{\tau_z}[\text{linac-bunch}] = 2\frac{1}{\tau_z}[\text{circulating-bunch}], \tag{12}$$

and the effective bunch length is $\sigma_z = \frac{1}{\sqrt{2\pi}} c\Delta t$, where Δt is the slice duration.

Each slice is assumed to be Gaussian distributed in transverse coordinates and energy spread, and to be uniformly distributed in the longitudinal direction. The Bjorken-Mtingwa formula is used to calculate the growth rate τ_d locally and is integrated over the entire section for each slice. At the end of the section (just prior to the location of the next IBSCATTER element), particles in each slice are scattered smoothly or randomly based on the calculated τ_d.

Particles are then put back together as a whole bunch, and all is ready for simulation of the next section of beamline.

We applied this method to the same APS ERL lattice used for our Touschek studies. Figure 13 shows the IBS growth rate with and without slicing beam. It's clear that the IBS growth rate of each slice is higher than if calculated for the whole bunch, especially in the longitudinal direction.
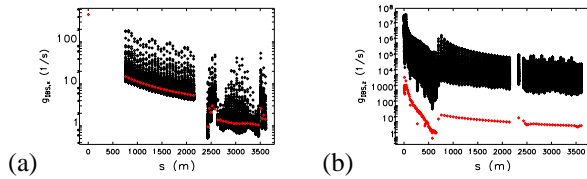

(a)   (b)

Figure 13: IBS growth rate for sliced bunch (black, each dot represents a slice) and unsliced bunch (red): (a) τ_x, (b) τ_z.

Figure 13 also shows that the longitudinal IBS growth rate is much higher than the transverse growth rate; this is expected due to the fact that the beam is much cooler in the longitudinal dimension. Figure 14 shows the beam dimensions at the end of the linac with (77 pC) and without (0 pC) IBS effect. There is no noticeable change in the transverse dimension. In the longitudinal, the energy spread at the center of the bunch increases due to the IBS effect. The change of energy spread is small and mainly happens at the center of the bunch. There should be no significant effect on brightness or FEL gain. It is possible that it may reduce CSR effects. Figure 15 shows the evaluation of energy spread of the entire bunch. There is no noticeable difference with and without the IBS effect.
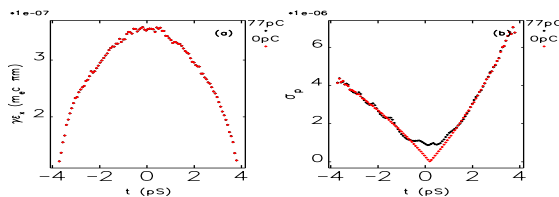

Figure 14: Particle distribution vs. longitudinal position (t) at the end of beamline with/without IBS: (a) normalized emittance; (b) energy spread.
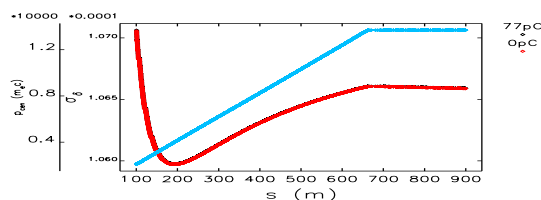

Figure 15: Bunch energy spread evolution vs. s.

CONCLUSION

We developed a method based on `elegant` to simulate beam-scattering effects for a linac beam with energy variation. The beam loss rate and location can be obtained by tracking scattered particles from Monte Carlo simulation, using realistic beam distributions. Beam-size evaluation is obtained by applying the Bjorken-Mtingwa formula to a sliced bunch. After applying the tools to an example APS ERL lattice design, we found that the Touschek scattering effect is significant. The momentum aperture of the lattice needs to be optimized carefully, and a beam collimation system can be designed based on the simulation results. The IBS growth rate is also very high for such a beam, but due to the fact that the time to travel through the linac is very short, the IBS effect has not enough time to develop. Hence there is no obvious effect on the machine's performance.

REFERENCES

[1] M. Borland, "elegant: A Flexible SDDS-Compliant Code for Accelerator Simulation," Advanced Photon Source LS-287, April 2000.

[2] J.D. Bjorken, S.K. Mtingwa, "Intrabeam Scattering," Part. Acc. 13 (1983) 115. 2000.

[3] M. Borland and A. Xiao, Proc. of PAC'07, 3453 (2007); www.JACoW.org.

[4] A. Xiao, Proc. of LINAC08, Victoria, Canada, to be published at www.JACoW.org.

[5] M. Borland and A. Xiao, Proc. of LINAC08, Victoria, Canada, to be published at www.JACoW.org.

[6] M. Borland and A. Xiao, Proc. of PAC'09, Vancouver, Canada, to be published at www.JACoW.org.

[7] M. Borland et al., Proc. of AccApp'07, 196 (2007).

[8] X. Dong, private communication.

[9] G. Hoffstaetter, M. P. Ehrlichman and A. Temnykh, Proc. of EPAC08, 1631 (2008); www.JACoW.org.

[10] W. T. Ford, A. K. Mann and T. Y. Ling, "Beam Polarization Effects in High Energy Electron-Positron Storage Rings," SLAC-158, 1972.

[11] A. Piwinski, "The Touschek effect in strong focusing storage rings," DESY 98-179, Nov. 1998.

[12] A. Piwinski, "Intra-beam Scattering," CERN Accelerator School, p. 226 (1991).

[13] S. Khan, "Simulation of the Touschek Effect for BESSY II: A Monte Carlo Approach," Proc. of EPAC94, 1192 (1994); www.JACoW.org.

[14] S. Khan, private communication.

[15] F. Zimmermann, "Intrabeam scattering with Non-Ultrarelativistic Corrections and Vertical Dispersion for MAD-X," CERN-AB-2006-002, Jan. 2006.

Multi-Particle Beam Dynamics